NASA

Technical Memorandum 81985

Quasi-Simultaneous Observations of the BL Lac Object MK 501 in X-Ray, UV, Visible, IR and Radio Frequencies

Y. Kondo, D. M. Worrall, R. F. Mushotzky, R. L. Hackney, K. H. Hackney, J. B. Oke, H. Yee, G. Neugebauer, K. Matthews, P. A. Feldman and R. L. Brown

JULY 1980

National Aeronautics and Space Administration

Goddard Space Flight Center
Greenbelt, Maryland 20771

QUASI-SIMULTANEOUS OBSERVATIONS OF THE BL LAC OBJECT MK 501 IN X-RAY, UV, VISIBLE, IR AND RADIO FREQUENCIES

Y. Kondo
Laboratory for Astronomy and Solar Physics

and

D.M. Worrall[1] and R.F. Mushotzky
Laboratory for High Energy Astrophysics
NASA/Goddard Space Flight Center
Greenbelt, Maryland 20771

R.L. Hackney and K.R.H. Hackney
Department of Physics & Astronomy
Western Kentucky University

J.B. Oke and H. Lee
G. Neugebauer and K. Matthews
Palomar Observatory[2]
California Institute of Technology

P.A. Feldman
Herzberg Institute of Astrophysics
NRC of Canada, Ottawa

Robert L. Brown
National Radio Astronomy Observatory[3]
Green Bank

[1]Also University of Maryland. Now at University of California, San Diego

[2]Observations were also made at the Mt. Wilson Observatory as part of a collaboration between California Institute of Technology and Carnegie Institution of Washington.

[3]Operated by Associated Universities, Inc., under contract with the National Science Foundation

ABSTRACT

Quasi-simultaneous observations of the BL Lac object MK 501 were performed for the first time at X-ray, ultraviolet, visible, infrared and radio frequencies. As the BL Lac objects are known to vary in their flux, such a "quasi-instantaneous" spectral energy profile is necessary in order to describe properly the energy generation mechanism. The observed spectral slope from the X-ray to UV regions is positive and continuous, but that from the mid-UV to visible light region becomes gradually flat and possibly turns down toward lower frequencies; the optical-radio emission can not be accounted for by a single power law. Several theoretical models have been considered for the emission mechanism. In some cases quantitative comparison with the data is not practical. However, most of the models are, at least, not inconsistent with the observations. A quantitative comparison has been performed with the synchroton-self-Compton model; the total spectrum is found consistent with this model. The spectrum from visible light to X-ray is consistent with synchrotron radiation or with inverse-Compton scattering by a hot thermal cloud of electrons. The continuity of the spectral slope from X-ray to UV implied by the current data suggests that the previous estimates of the total luminosity of this BL Lac object has been underestimated by a factor of about three or four.

I. INTRODUCTION

BL Lacertae objects share a number of properties in common with quasars and, as a consequence, are generally considered to be closely related to quasars. Features of BL Lac objects by which they are often distinguished from "average quasars" are as follows. Many BL Lac objects have been located in the cores of elliptical galaxies; the spectrum of the core region exhibits little or no detectable line emission indicating a virtual absence of gas; the optical and radio emissions are highly linearly polarized; the fluxes vary significantly at all wavelengths.

Relatively larger and more rapid changes have been observed in visible light and in the near-infrared regions than at the radio wavelengths. In visible light, variations have been observed on a time scale on the order of 10 days (Stein, O'Dell and Strittmatter 1976). Based on archival plates, there are apparently quiescent and active phases in some sources, which may brighten by as much as some 5 magnitudes during the active phase. Variability in the ultraviolet and X-ray regions is currently being investigated using the satellite observatories. In the case of MK 421, the 2-10 keV X-ray flux was observed to change by an order of magnitude on the time scale of days (Ricketts, Cooke and Pounds 1976). Modulation collimator experiments have recently verified and established unambiguously the following five BL Lac objects as X-ray sources: MK 501, MK 421, PKS 0548-322, PKS 2155-304 and 2A 1219+305 (Hearn, Marshall and Jernigan 1979; Schwartz et al. 1978, 1979).

It is generally suspected that the energy generation mechanism in quasars is the same as that in BL Lac objects. Since the spectrum of a BL Lac object is relatively uncontaminated by the spectrum of gas, the physical mechanism for the non-thermal radiation in both types of source may be investigated effectively by observing BL Lac objects. These observations must be made on a timescale short compared to the characteristic timescale for variation of the source. Observations of both the flux and polarization of 12 BL Lac objects by

Angel et al. (1978) suggest that the shortest characteristic timescale for the erratic variability seen in some objects is $\gtrsim$ 1 day. Similarly, in the X-ray, the shortest observed timescales for a BL Lac object, PKS 2155-304 (Snyder et al. 1980) is approximately one day. However such rapid variability has not been detected in MK 501. For this object no variability has been reported at radio frequencies and the variability at visual wavelengths reported by Barbieri and Romano (1977) occurred on a timescale of years with a range of .9 mag.

Our present observations indicate that the X-ray variability also occurs on timescales longer then one week since no significant intensity change was seen during each of our 6 day observation periods while significant spectral changes were seen over a 6 month timescale. We therefore consider the radio, infrared, optical, ultraviolet and X-ray observations reported in this paper to represent a quasi-simultaneous "snapshot" of the total spectrum of MK 501.

II. OBSERVATIONS

The data discussed in this work were obtained in August and September 1978 with the HEAO-1 and IUE satellites, the 5-meter and 2.5-meter telescopes at the Hale Observatories, the NRAO 92-meter radio telescaope at Green Bank, and the 46-meter radio telescope at the Algonquin Observatory.

The X-ray measurements were made with the A2 experiment on the HEAO-1 spacecraft. The detectors are comprised of mechanically collimated gas-filled multi-wire proportional counters (see Rothschild et al. 1979 for the experiment description). Measurements were made with the argon and xenon-filled counters. For a spectral determination in the 2-50 keV range, MK 501 was observed in a pointing maneuver of the satellite between 1978 September 8 19:00 and September 9 01:00 UT corresponding to JD 2443760.29 and JD 2443760.54. Net source counts were obtained by subtracting background counts accumulated from a region close to the source which the detectors were scanning between 1978 August 21 and August 31 UT. During this scanning period, MK 501 was in view for about 1 minute every 30 minutes, enabling its intensity to be monitored throughout the interval.

The IUE instrumentation has been described by Boggess et al. (1978). For this program, spectral observations of MK 501 were made in the low-dispersion mode (effective resolution $\lesssim$ 10 Å) using the optimally configured SWP (short-wave length prime) and LWR (long-wavelength redundant) cameras. The total frequency (ν) range observed was $14.97 < \log \nu < 15.36$. MK 501 was observed using the 10 x 20 arc sec aperture to insure acquisition by blind offset and to permit application of the flux calibration which is appropriate for this focal-plane aperture. The cameras were prepared using both the XPREP sequence (to erase all traces of previous over-exposures) and the SPRFP sequence (to minimize the unexposed background level). The short-wavelength spectral image SWP 2394, covering the range between 1275 and 1910 Å, was obtained 1978 August 25 03:22 - 09:42 UT; the region shortward of 1275 Å was contaminated by geocoronal and interplanetary Lyman-α emission. The long-wavelength spectral image LWR 2177, ranging from 1900 to 3140 Å, was obtained 1978 August 26 03:12 - 08:12 UT. Both IUE exposures were made during the lowest-radiation part of the IUE orbit. Under these conditions, the radiation-contributed background over the relatively long exposure times amounted to approximately one-quarter the total response at the wavelengths of peak sensitivity of the cameras. The effective signal-to-noise ratio for single data elements (2 Å bandwidth SWP, 4 Å bandwidth LWR) indicated by the standard deviation of the measurements of net signal after subtraction of the smoothed background is typically about 12:1.

The 5-meter Hale telescope observations were made using the multichannel spectrometer for visible light with an aperture size of 10 arc seconds. The frequency range covered was $14.42 < \log \nu < 14.96$, with 40 Å bandpasses for $\lambda <$ 5700 Å and 80 Å for $\lambda >$ 5700 Å. Similar observations were obtained on the following dates: 1978 May 26 9:25; 1978 Aug. 29 4:15; 1978 Aug. 30 3:39; and 1978 Aug. 31 3:34 UT.

The infrared observation at Mt. Wilson was made with the 2.5-meter telescope at 2.2 μm ($\Delta\lambda$ = 0.4 μm) on 1978 August 31 03:08 UT. The aperture was 15 arc seconds in diameter.

Observations with the 46-meter telescope of the Algonquin Radio Observatory*

*The Algonquin Radio Observatory is operated by the National Research Council of Canada, Ottawa, as a national radio astronomy facility.

were made at 10275 MHz (log ν = 10.02) (1978 August 15-24 UT) and 10650 MHz (log ν = 10.03) (1978 August 30 - September 3 UT), using a beam-switched receiver with system temperature of about 150 K and bandwidth of approximately 100 MHz.

The 92-meter radio telescope observations at Green Bank were obtained on most days in the period 1978 August 15-31 at source transit (between 12:00 and 13:00 UT). The frequency used was 4750 MHz (log ν = 9.68); the system temperature was 70 K and the instantaneous continuum bandwidth was 500 MHz.

III. REDUCTION AND DESCRIPTION OF THE DATA

A. X-Ray Spectrum (HEAO-1)

The X-ray spectrum was derived from the HEAO-A2 pointing observation between 1978 September 8 19:00 and September 9 01:00 UT. The spectrum is soft enough for the best statistical accuracy to be achieved with the argon detector. The upper portion of Figure 1 shows the incident counts along with the best model fit. Xenon detector data give consistent spectral fits. Figure 1 also shows the inferred incident spectrum after folding through the detector response. The best value for the index of the differential photon spectrum, Γ, is $\sim$ 2.52 and the best fit low energy absorption implies a column density, N_H, of $\sim 4.6 \times 10^{21}$ atoms cm^{-2}. In this paper we use α for the slope of a power law fit to the continuum such that the flux at a given frequency f_ν is defined as $f_\nu = A\nu^{-\alpha}$ (Wm^{-2} Hz^{-1}). The photon index Γ, is related to the energy index α by $\Gamma = \alpha + 1$. The X-ray spectra are fitted to a form $f_\nu = A\nu^{-\Gamma}\exp(-\sigma N_H)$ ph cm^{-2} sec^{-1} keV^{-1} where N_H is the equivalent column density of hydrogen atoms assuming that the material is neutral and σ is the appropriate cross section (Fireman 1974). The

90% confidence error contour for Γ and N_H is also shown in the figure. No additional structure to the spectral form significantly improves χ^2. A thermal bremsstrahlung fit is found to give a worse χ^2, although one which is acceptable at 70% confidence limit. The best temperature in this case is 4.5 keV.

In the HEAO-1 nominal scanning mode, the spin axis points towards the sun, thus moving a degree each day, and the A2 detectors take $\sim$ 30 minutes to trace each great circle on the sky. MK 501 is at fairly high ecliptic latitude and so was in view for about one minute during each scan for 10 days (1978 August 21-31). The coverage is very incomplete because of pointing operations at other regions of the sky for several periods of 8-12 hours during this time. There are too few counts to enable spectral parameters to be determined with sufficient precision to discern any spectral change between this period and that in September.

For the pointing observation, the 2-6 keV and 2-20 keV energy fluxes are $(2.9^{+1.0}_{-0.5}) \times 10^{-11}$ erg cm^{-2}s^{-1} and $(4.5^{+2.9}_{-1.3}) \times 10^{-11}$ erg cm^{-2}s^{-1}, respectively. Experimental systematic effects and the unavoidable presence of intrinsic sky fluctuations dominate the quoted errors. The average intensity from scanning data can be determined with comparable precision and is found to be in agreement. Furthermore, one-quarter day averages for the August scanning observations are consistent with a constant flux to within 60% confidence.

If we compare our observations with previous X-ray observations of MK 501, we find no evidence so far for changes in the 2-6 keV energy flux. The revised UHURU value of $(2.75 \pm .52) \times 10^{-11}$ erg cm^{-2}s^{-1} (Forman et al. 1978), the August 1977 HEAO-A3 value of $(3.6 \pm 1.2) \times 10^{-11}$ erg cm^{-2}s^{-1} (Schwartz et al. 1978) and the March 1975 Ariel 5 value of $(3.6 \pm 1.8) \times 10^{-11}$ erg cm^{-2} s^{-1} (Snijders et al. 1979) are comparable to the present value. Simultaneously with the A3 measurement, the A2 detectors observed the source in August 1977 (Mushotzky et al. 1978; Mason et al. 1979). The 2-6 keV flux agreed with the A3 value and hence with the present one. However, the spectrum was of a different form. A single value of Γ, as defined earlier, did not give an acceptable fit to the

data. A photon index $\Gamma \simeq 2.5$ from 0.15 to 3 keV, with a hardening to about 1.2 above 3 keV, was required. Mason et al. (1979) suggest that this two component nature may also be present in MK 421. They interpret the large spectral and intensity change in MK 421 which occurred over 6 months (Mushotzky et al. 1979) as due to variability of the hard component by about a factor of 5, combined with a relatively constant low energy component which extends from 2 keV to lower energies. The present MK 501 observation suggests that this object also may always be characterized by two components, where both are seen to change in intensity. The suggestion is that between August 1977 and August 1978 the hard power law component with $\Gamma \sim 1.2$ decreased by about a factor of two in intensity while the soft component with $\Gamma \sim 2.5$ increased by a similar factor. The 1.2 - 12 keV Ariel 5 data were shown by Snijders et al. (1979) to be inconsistent at 90% confidence with single power laws of slope less than 1.2 or greater than 2.3, and gave $\Gamma = 1.8 \pm 0.5$ as the best fit. However, these authors have not considered a two-power law fit. Inspection of their data would not appear to rule out such a possibility, in which variability of the two components would be suggested. While it is premature to draw strong conclusions, we tentatively suggest that BL Lacertae objects as a class are characterized by such multiple component X-ray spectra, where the overlap is seen at a few keV. In contrast, when the 2-50 keV flux from the quasar 3C 273 was examined for spectral changes accompanying the intensity changes discerned over a few months, none were found at a confidence level comparable to those reported here for spectral changes in MK 501 (Worrall et al. 1979).

B. Ultraviolet Spectrum (IUE)

The IUE data for MK 501 were calibrated to absolute fluxes using the calibration established by Bohlin et al. (1979). Additionally, special observations of calibration stars were required for deriving corrections specific

to the MK 501 exposure conditions to remove effects introduced by an erroneous photometric intensity transfer function used for processing SWP images prior to 1979 July. The calibrations and the image processing procedures are continually subject to evaluation and possible revision as the observing experience with the IUE instrumentation progresses. Uncertainties in the calibrations are currently estimated to be no greater than about $\pm$ 15%.

Calibrated data from IUE exposures SWP 2394 and LWR 2177 are listed in Table 1 and plotted in Figure 2. Individual data samples have been binned into larger wavelength intervals to increase the effective signal-to-noise ratio for determining local continuum levels. Included measurements cover ranges of 3140 - 1900 Å (LWR camera) and 1910 - 1275 Å (SWP camera). No discrete spectral features of the source were evident in the fully resolved data set, for which the detection limit is estimated to be $\sim$ 4 Å in equivalent width.

A heavily exposed IUE observation of the BL Lac object MK 421 which, like MK 501, has a detectable galactic envelope in visible wavelengths, revealed no evidence of flux from the surrounding galaxy in the wavelength range of the LWR camera (3200 - 1900 Å). Thus, we feel that the IUE spectra of MK 501 are essentially due only to the compact nuclear BL Lac source with little contribution from the associated galaxy.

In Figure 2 are plotted the IUE data both before and after the application of a correction for effects of interstellar reddening. Since no direct determination of reddening is available for MK 501, the mean color excess E(B-V) = 0.083 mag appropriate to its galactic latitude was adopted as the basis for applying the ultraviolet extinction curve of Code et al. (1976). The 2170 Å extinction feature is not significantly detectable in our observation with a substantially better signal-to-noise ratio than that of the short-exposure data used by Snijders et al. (1979). The weakness of this feature suggests that E(B-V) is less than 0.1 mag in the direction of MK 501. Snijders et al. adopted a larger value for the color excess in order to minimize an apparent depression

near the center of their IUE spectrum. For our calibrated and dereddened spectra, we obtain the following power-law indices (in the sense $f_\nu \propto \nu^{-\alpha}$):

LWR	$\alpha = 0.31 \pm 0.23$	(3140 - 1900 Å)
SWP	$\alpha = 1.23 \pm 0.35$	(1910 - 1275 Å)
LWR + SWP	$\alpha = 1.02 \pm 0.14$	(3140 - 1275 Å)

The quoted errors are 95% confidence limits for the power-law indices estimated on the basis of the internal error of the data sets; they do not include the uncertainties in either the reddening correction or the calibrations. If the appropriate E(B-V) is actually less than the adopted value of 0.083 mag, then the ultraviolet continuum of the source is steeper than indicated by the results here reported. The degree of possible reddening of the BL Lac source due to its surrounding galaxy is also unknown. The significant difference between the indices of power laws fitted to the separate LWR and SWP data sets is interpreted as being due to a curvature of the spectral energy distribution, with a turnover toward longer wavelengths. These results differ significantly from the $\alpha = 0.50^{+0.10}_{-0.15}$ result of Snijders et al. (1979) for the total UV spectrum.

C. Visible Light Spectrum (5-Meter Telescope)

All the observations give the same magnitude (V = 13.75) and energy distribution. A typical spectral scan is shown in Figure 3. The spectrum clearly contains a galaxy, as one can see the H and K Ca II break, the depressions at 4150 Å, 4300 Å, the Mg-b band, and effects of bands in the red. A match up with a standard elliptical galaxy yields the redshift $z = 0.034 \pm 0.002$. The energy distribution is flatter than a normal elliptical and the H and K lines are abnormally weak, as is typical of galaxies with a nonthermal blue continuum.

A model fitting procedure was performed by adding a normal elliptical galaxy energy distribution (Yee and Oke 1978) to a power law of index α. There are no reasonable fits when α is +1.0 or +0.5. The best fit occurs with $\alpha = 0$; but $\alpha = -0.5$ is also possible. A very small reddening correction corresponding to $E_{B-V} = 0.05$ is applied.

Fits are all given in terms of visual magnitude and for $\alpha = 0$. For the 10 arc second aperture the non-thermal part has $m_v = 15.11$, which corresponds to 0.33×10^{-28} W m^{-2} Hz^{-1}. The galaxy part has $m_v = 13.94$ or 0.95×10^{-28} W m^{-2} Hz^{-1}. For $H_o = 55$ km s^{-1} Mpc^{-1} and $q_o = 0$, the absolute visual magnitude of the galaxy is -22.3 within a 10 arcsecond diameter aperture. The galaxy appears to be highly concentrated towards the center since the magnitude difference for a 7" and 10" aperture is only 0.18 mag. Thus the total absolute visual magnitude of the galaxy is perhaps -22.5 to -22.8; the galaxy is therefore of only modest luminosity.

Previous measurements of the continuum by Maza, Martin and Angel (1978) indicate that the polarized continuum radiation has a slope $\alpha = 0.83 \pm 0.10$, considerably steeper than the fit to the continuum derived here. This fit is similar to the overall fit to our UV data. This suggests that the non-thermal component has varied between the epoch of Maza et al. and the present observations. Comparisons of fluxes in the V, B and U bands (log $\nu \sim$ 14.73, 14.83, and 14.92 respectively) show a possible change in the B flux from Maza et al.'s value of log F_ν = -28.02 W m^{-2} Hz^{-1} to our value of log F_ν = -28.19 (see Figure 5 of Maza et al. and Figure 3 of this paper), while the V and U fluxes were the same. We also note that Maza et al.'s values of U-B, B-V, and U-B differ from those of Tapia, Craine, and Johnson (1976) thus giving further evidence for optical intensity and spectral variability.

D. Infrared Data (2.5 Meter Telescope)

The procedures for the data reduction are as described by Neugebauer et al. (1978).

The measurement at 2.2 μm at 15" diameter aperture yielded a flux value of 35 ± 3 m Jy or M_K = 10.6 ± 0.1 where the error indicated is 1σ. If the galaxy part of the visual light is extrapolated to a 15" aperture using the same curve of growth that exists between 7" and 10", then m_v = 13.75. This produces a color in close agreement with the average value of V-K = 3.3 for elliptical galaxies found by Frogel et al. (1978). If allowance is made for the uncertainties in the photometry and the extrapolation to m_v and, also, if V-K = 3.0 is taken as a lower limit for elliptical galaxies, then roughly one half of the 2.2 μm flux in a 15" aperture could be non-thermal. This produces a lower limit of $\alpha \gtrsim 1.2$ between 0.5 and 2.2 μm. This limit on α is consistent with the value of α derived in this paper from the visual data and α = .82 between 0.44 and 10.6 μm found by Ulrich et al. (1975).

E. Radio Data (46-Meter Telescope)

Throughout the period of the observations pointing corrections were checked, gain stability was monitored, and focus offsets were maintained by measurements of strong point calibration sources. Any residual pointing errors should not have exceeded about 20", which for the 2'40" beamwidth, corresponds to ∿ 5% of the measured flux density.

The observational results are plotted in Figure 5. Over the time interval 1978 August 15 - September 3 UT, there is no evidence for radio variability of MK 501, in agreement with the 92-meter observations at 4750 MHz. The mean flux densities are 1.14 ± 0.02 Jy at 10,275 MHz, 1.14 ± 0.01 Jy at 10,650 MHz, and 1.14 ± 0.01 Jy overall at 2.85 cm, where the errors quoted are at 2σ. These results are identical, within experimental error, to earlier measurements at 2.8 cm (see, e.g., McCutcheon and Gregory 1978).

F. Radio Data (92-Meter Telescope)

The results of the radio data at 4750 MHz are plotted in Figure 4. The error bars are $\pm 2\sigma$. Over the time interval of these observations the source was quiescent. The mean flux density is 1.327 Jy, a value in keeping with the value of 1.295 Jy interpolated at this frequency from the observations at 2.6 and 8.1 GHz made by Sramek and Toumassian (1976).

IV. DISCUSSION OF OBSERVATIONAL RESULTS

Constraints from the Overall Spectrum

We have plotted all of the quasi-simultaneous data for MK 501 in Figure 6. As was discussed earlier, it is probably safe to assume that the contribution of photons from the galaxy is negligible to the X-ray and ultraviolet data. In visible light there is a substantial contribution from the galaxy. We have therefore plotted both the observed flux (galaxy and the BL Lac source combined) and the deduced BL Lac source flux; the former is indicated by a line and the latter by a broad bar. No correction for the galaxy light can be made for the IR data at the moment. The radio flux may be considered to be basically all from the BL Lac source.

The most significant feature in the observed spectral energy distribution is the turnover from the UV into the visible light component. We should also note that although there exists an apparent continuation of the slope from the UV to the X-ray region, the slope for the intervening region ($\alpha \simeq 0.9$) fits the UV data but not that within the observed X-ray band. We infer a steepening of the slope at X-ray wavelengths, which is possibly related to the electron energy loss mechanism in the source.

Various emission mechanisms have been proposed for the BL Lac sources, including synchrotron self-Compton emission (Jones, O'Dell and Stein 1974b), Compton emission (scattering) from thermal electrons (Katz 1976), bremsstrahlung emission from accretion disks (Eardley et al. 1978), and emission from turbulent

plasmas (Colgate et al. 1975) or hot gas clouds (Fabian et al. 1976; Schnopper et al. 1977). We shall concentrate on the first two mechanisms because they have been presented in forms amenable to quantitative assessment.

A. Synchrotron Self-Compton Emission

Two features of the total flux density spectrum (Fig. 6) are immediately suggestive of a synchrotron self-Compton model for the radio and visible-light, ultraviolet, X-ray emission from MK 501: these are (1) the flattening or turn-over in the radio spectrum at $\nu \cong 10$ GHz [see Schwartz et al. (1978) for a more complete representation of the radio spectrum] and (2) the corresponding flattening in the visible light at $\nu \cong 10^{15}$ Hz. This is precisely the shape of the total synchrotron self-Compton spectrum expected from a source in which the radio emission is synchrotron radiation while the visible light, ultraviolet and X-ray emission (all frequencies $\sim 10^{14} - 10^{18}$ Hz) is first-order Compton scattering of the relativistic electrons with the radio photons (Jones et al. 1974a, 1974b; Burbidge et al. 1974). Since definite relationships exist between the synchrotron and Compton components we can readily investigate the consistency of this model in the particular case of MK 501.

The first-order Compton flux density can be expressed in terms of the observable radio properties of the assumed spherical, isotropic and homogenous source (Marscher et al. 1979) as

$$S_c(\nu) \cong 10^{-4} K_s(\alpha) \ln \frac{\nu_2}{\nu_m} S_m^{2(\alpha+2)} \theta^{-2(\alpha+2)} \nu_m^{-(3\alpha+5)}$$

$$\times \left[\frac{\nu_x}{2.4 \times 10^{17}}\right]^{-\alpha} \times 10^{-26} \text{ W cm}^{-2}\text{s}^{-1}\text{Hz}^{-1},$$

where K_s is a function tabulated by Marscher et al. (1979) and is of order 1. Here, ν_2 is the upper frequency limit of the synchrotron radio spectrum, ν_m(GHz) is the frequency where the radio flux density is maximum, S_m(Jy) is the radio flux density at ν_m, θ (milliarcsec) is the angular diameter of the

source and ν_x(Hz) is the frequency of the first-order Compton scattered photons. For a consideration of the effects of relativistic motion and non-homogenity, see Gould (1979) and Jones, O'Dell and Stein (1974a). For the rest of this discussion we shall assume such effects are small. The spectral index used in this expression, α is the spectral index of the optically thin radio spectrum which is difficult to establish because the source appears at least partially optically thick at all frequencies less than 10 GHz (i.e., the radio spectrum is flat at these frequencies). However, in the synchrotron self-Compton model, the optically thin synchrotron spectral index is identical to the Compton spectral index and this latter quantity we can establish from our (Fig. 6) UV and X-ray flux densities as $\alpha \simeq 0.9$. This value is different from the local index in either the UV or the X-ray band and is appropriate for an UV-X-ray index. But, our result is insensitive to the exact values of the spectral index α. Using this value of the spectral index together with the angular diameter of the radio core of MK 501 as measured by VLBI techniques at 6 cm, θ = 1.1 mas (Weiler and Johnston 1980), R $\approx$ 3.4 l.y., and the extrapolated maximum flux density $S_m \cong$ 2 Jy at a turnover frequency of the core, $\nu_m \cong$ 2 GHz, we obtain an X-ray flux of

$$S_c\,(10^{18}\ \mathrm{Hz}) \cong 2.2 \times 10^{32}\ \mathrm{W\ m^{-2}\ Hz^{-1}},$$

which is in good agreement with the observations. The magnetic field strength is also determined in this model,

$$B = 3.4 \times 10^{-5}\ \theta^4\ \nu_m^{\,5}\ S_m^{-2} \cong 4.0 \times 10^{-4}\ \mathrm{G}.$$

The flattening of the first-order Compton emission that appears at visible light wavelengths can be accounted for as a low energy break or turnover in the Compton spectrum. Briefly, if the power law distribution of relativistic electrons has a low energy cutoff at an energy E_1, then the self-Compton radiation spectrum will reflect this cutoff at a frequency

$$\nu_c' \cong \frac{4}{3}\left(\frac{E_1}{mc^2}\right)^2 \nu_m.$$

For MK 501 if $\nu_c' \cong 10^{15}$ Hz, then $E_1 \cong 310$ MeV. These electrons will radiate synchrotron emission at 200 MHz and are therefore not accessible to direct observation in the radio spectrum (see Marscher 1977) for a description of the detailed spectrum for this case). The first order Compton radiation will extend from $\sim 10^{15}$ Hz to an upper frequency limit ν_c^2, which is determined by the high energy cutoff of the distribution of relativistic electrons. Let this high energy limit be E_2, then,

$$\nu_c^2 \cong \frac{4}{3} \left[\frac{E_2}{mc^2} \right]^2 \nu_2 .$$

Choosing ν_2 conservatively as the highest frequency at which radio emission has been detected from MK 501, $\nu_2 = 100$ GHz (Joyce and Simon 1976) we find that $E_2 \cong 4$ GeV (from the synchrotron critical frequency in a field of 4×10^{-4} G) and hence that $\nu_c^2 \cong 8 \times 10^{18}$ Hz. At frequencies near ν_c^2 we expect the spectral index to begin to steepen; the X-ray data are consistent with this predicted steepening.

Finally, the total self-Compton luminosity 10^{15} - 10^{19} Hz is $L_c \cong 5.5 \times 10^{45}$ ergs s^{-1} assuming that the distance to MK 501 is $\sim$ 200 Mpc as given by the redshift ($z = 0.0337$ (Ulrich et al. 1975) and $z = 0.036 \pm 0.002$ (present work)) with $H_0 = 55$ km s^{-1} Mpc^{-1}. The energy density in relativistic electrons is

$$u_e \cong 1.6 \times 10^{-2} \; \theta^{-9} \; \nu_m^{-7} \; S_m^4 \cong 8.2 \times 10^{-3} \text{ erg cm}^{-3},$$

which means that the total energy in relativistic electrons is $U_e \cong 1.2 \times 10^{54}$ ergs and the resultant lifetime of the radiating particles $\tau \cong U_e/L_e \cong 6.8$ years. This timescale compares favorably with the timescale for X-ray variability (Mushotzky et al. 1979).

The lifetime for spectral variability in the X-ray can be estimated from the effects of synchrotron and Compton losses on the electron spectrum. The lifetime for synchrotron emitting electrons whose Compton scattered photons are observed at 5 keV is $\sim 4 \times 10^3$ years, while the Compton loss lifetime is $\sim$ 4 years. The high frequency break in the photon spectrum caused by Compton losses appears at $\nu_B = 3.6 \times 10^{13}\ t^{-2}$ Hz, where t is the time after injection in years. So, the spectrum is expected to break in the far IR region. As the preceding equation shows, the lifetime is a very sensitive function of θ and ν_m and the fact that the calculated lifetimes approximately agree with the observations is somewhat fortuitous.

We note that our solutions differ significantly from the similar calculations of Schwartz et al. (1978). This is primarily due to the recent angular size data of Weiler and Johnson (1980) and reflects the problems inherent in deconvolving radio spectra composed of multiple components.

B. Inverse-Compton Scattering Off Thermal Electrons

The apparent continuation of the power law between the visible light and X-ray regions suggests that the mechanism discussed by Katz (1976) may be appropriate for the source. In his model sion is due to Compton scattering. The origin of the initial supply of soft photons is not explained. The electrons originate in a hot gas cloud and have non-relativistic velocities. Radiation is restricted to below a few hundred keV since the Comptonized photons must have energy less than that of the non-relativistic electron gas. A fit to the observed spectral slope, allowing variability by as much as a 25% change in flux in a period over the order of one year, gives an electron density $\gtrsim 10^8$ cm^{-3} and a source size $\lesssim$ 0.3 light years. The mass necessary to bind the gas cloud at the limit of maximum source size is $\sim 3 \cdot 10^6\ M_\odot$.

C. Synchrotron Radiation

The appearance of a "break" by approximately one unit in the visible-light-UV spectrum and the extension of that "broken" power law into the X-ray band suggests synchrotron radiation as the source of the visible-light-UV-X-ray

continuum. In this model the radio flux would be from a different, presumably larger component. If we regard the "break" as being due to synchrotron energy losses and use $\nu_B \sim 1.5 \times 10^{15}$ Hz one derives $B \sim 6 \times 10^{-3}\ t_{yr}^{3/2}$ gauss. In a synchrotron model the two other interesting parameters are its size, R and the particle density, N_o such that $N_o\ \gamma^{-n}\ d\gamma = n(\gamma)\ d\gamma$. We can take the standard synchrotron emissivity formula and derive the product $R^3 \times n_o$. For MK 501 we derive $R^3\ n_o \sim 4.2 \times 10^3$. In this type of model the loss times scale as $\nu^{1/2}$; so, one might expect the X-ray to be more variable then the visible-light or UV.

D. Other Possibilities

1. Emission from an Accretion Disk Around a Black Hole

The spectral energy distribution in this case depends heavily upon a number of assumptions regarding the physical parameters involved. The calculations currently available (Eardley et al. 1978) are limited to a black-holes of mass 100 M_o and 10.0 M_o. The spectral turnover predicted by these authors for their standard disk and two-temperature disk models typically occurs in the far ultra-violet, while an optically thin model predicts no spectral turnover. Comparing the calculations for $M_{\text{black-hole}}$ = 100 M_o and 10 M_o shows that the turnover point shifts toward longer wavelengths as the mass of the black-hole is increased, suggesting the possibility that for sufficiently large mass, the turnover may occur in ultra-violet or visible light. In order to account for the radio flux, however, another component (e.g., synchrotron emission) is needed in addition to the bremsstrahlung component. Further theoretical calculations are needed to extend the model to include masses for which the turnover occur in optical frequencies.

2. Emission from Acceleration Limited Radiation

Recently Cavaliere and Morrison (1980) have calculated the emission from a source where continuous reacceleration is taking place. In this model, visible light and UV emission can be characterized by $F_\nu = A_\nu^{-\alpha}$ where $\alpha = (m-1)/(m-a)$, in which the magnetic field B has a radial dependence $B = B_o\ (r/R)^{-m}$ and $P(r) = P_o\ (r/R)^{-a}$ is the radial dependence of the energy gain of a particle. There are 3 possible higher energy components of slopes $s = 1/(2m-a)$, or $1/(2-a)$, or $1/a$

depending on the dominant region in the model. If we let α be set by the radio emission and δ by the X-ray we derive $m = 1$, $a = 1$, for all 3 cases. Thus the X-ray, UV and radio spectra uniquely define the radial dependences in this model.

V. CONCLUDING REMARKS

We have presented the first "quasi-instantaneous" spectral energy profile of the BL Lac source MK 501 and have compared it with predictions of two principal candidate emission mechanisms.

While the synchrotron self-Compton model is entirely consistent with our data and, as such, is a favored model, an unfortunate result of synchrotron self-Compton theory is that tight constraints on parameters cannot be achieved, as is evident from inspection of the relationships given in section IV (A).

A synchrotron origin for the optical-X-ray spectrum also might be reasonable.

Compton emission from thermal electrons can fit our data in the X-ray, ultraviolet and visible light regions, but we do have to assume an additional mechanism to account for the radio flux. The required size ($\sim$ light year) can be accommodated without necessarily assuming an exotic explanation such as a black hole. However, the source of soft photons needed for the Compton emission must also be explained.

We also do not rule out other mechanisms, although direct comparisons are presently not practical. In particular, an accretion disk surrounding a massive black hole giving rise to bremsstrahlung emission is a possibility to be further explored with theoretical calculations.

Since we are dealing with a variable source in all frequencies, with the possible exception of the radio, we may unravel the energy mechanism by again observing the source simultaneously in all frequencies when it is at a different flux level. Any change in the spectral energy profile will provide additional cludes for further constraining the model.

Since the UV and X-ray spectra imply continuity through the extreme UV to

soft X-ray, formal integration of this spectrum shows that most of the energy emitted by MK 501 appears in the extreme UV. This suggests that the previous estimates of the total luminosity has been underestimated by a factor of about three to four resulting in an integrated luminosity over our entire observed bandwidth of $\sim 1 \times 10^{45} \left(\frac{H_o}{50}\right)^{-3}$ erg s^{-1}.

The HEAO-A2 experiment is a collaborative effort led by E. Boldt of GSFC and G. Garmire of CIT with collaborators at GSFC, CIT, JPL and UCB. Thanks are due Dr. A. Boggess and the IUE Observatory staff at GSFC for their competent assistance in obtaining the data. Y.K., R.F.M., R.L.H. and K.R.H.H. are guest observers on the IUE. R.L.H. and K.R.H.H. gratefully acknowledge the assistance of W. Kinzel in the reduction of the IUE data and funding by NASA Grant NSG 5238 and the WKU Faculty Research Grant Committee. G.N. and K.M. acknowledge support by NASA. We thank A.D. Code for helpful discussions of the interstellar reddening and E.A. Boldt for valuable comments on the X-ray results. P.A.F. wishes to thank C.R. Purton, P.C. Gregory, and W.M. Turner for assistance with the observations at A.R.O.

REFERENCES

Angel, J.R.P. et al. 1978, Pittsburgh Conference on BL Lac Objects, ed. A.M. Wolfe, pg. 117, Univ. Pittsburgh Press.

Barbieri, C. and Romano, G. 1977, Acta Astron. 27, 195.

Boggess, A. et al. 1978, Nature 275, 387.

Bohlin, R.C., Holm, A.V., Savage, B.D., Snijders, M.A.J. and Sparks, W.M. 1979, NASA X-681-79-8.

Burbidge, G.R., Jones, T.W., and O'Dell, S.L. 1974, Ap. J. 193, 43.

Cavaliere, A. and Morrison, P. 1980, preprint.

Code, A.D., Davis, J., Bless, R.C., and Hanbury-Brown, R. 1976, Ap. J. 203, 417.

Colgate, S.A., Colvin, J.D., Petschek, A.G. 1975, Ap. J. (Letters) 197, L105.

Eardley, D.M., Lightman, A.P., Payne, D.G., and Shapiro, S.L. 1978, Ap. J. 224, 53.

Fabian, A.C., Maccagni, D., Rees, M.J. and Stoeger, W.R. 1976, Nature 260, 683.

Fireman, E.L. 1974, Ap. J. 187, 57.

Forman, W., Jones, C., Cominsky, L., Julien, P., Murray, S., Peters, G., Tananbaum, H. and Giacconi, R. 1978, Ap. J. Suppl. 38, 357.

Frogel, J.A., Persson, S.E., Aaronson, M., and Matthews, K. 1978, Ap. J. 220, 75.

Gould, R. 1979, Astron. Ap. 76, 306.

Hearn, D.R., Marshall, F.J., and Jernigan, J.G. 1979, Ap. J. (Letters) 227, L63.

Jones, T.W., O'Dell, S.L. and Stein, W.A. 1974a, Ap. J. 188, 353.

Jones, T.W., O'Dell, S.L. and Stein, W.A. 1974b, Ap. J. 192, 261.

Joyce, R. and Simon, M. 1976, P.A.S.P. 88, 870.

Katz, J.I. 1976, Ap. J. 206, 910.

Margon, B., Lampton, M., Bowyer, S., and Cruddace, R. 1975, Ap. J. 197, 25.

Marscher, A., Marshall, F.E., Mushotzky, R.F., Dent, W.A., Balone, K.T.J. and Hartman, M.F. 1979, Ap. J. 233, 498.

Marscher, A. 1977, Ap. J. 216, 244.

Mason, K., Reichert, G., Bowyer, S., Garmire, G. and Nugent, J. 1979, UCB preprint.

Maza, J., Martin, P.G., and Angel, J.R.P. 1978, Ap. J. 224, 368.

McCutcheon, W.H. and Gregory, P.C. 1978, A. J. 83, 566.

Mushotzky, R.F., Boldt, E.A., Holt, S.S., Pravdo, S.H., Serlemitsos, P.J., Swank, J.H., and Rothschild, R.H. 1978, Ap. J. (Letters) 226, L65.

Mushotzky, R.F., Boldt, E.A., Holt, S.S., and Serlemitsos, P.J. 1979, Ap. J. (Letters) 232, L17.

Neugebauer, G., Oke, J.B., Becklin, E.E. and Matthews, K. 1978, Ap. J. 230, 79.

Ricketts, M.J., Cooke, B.A., and Pounds, K.A. 1976, Nature 259, 546.

Rothschild, R.E. et al. 1979, Space Sci. Instrum. 4, 269.

Schnopper, H.W., Epstein, A., Delvaille, J.P., Tucker, W., Doxsey, R., Jernigan, S. 1977, Ap. J. (Letters) 215, L7.

Schwartz, D.A., Bradt, H.V., Doxsey, R.E., Griffiths, R.E., Gursky, H., Johnston, M.D., and Schwartz, J. 1978, Ap. J. (Letters) 224, L103.

Schwartz, D.A., Doxsey, R.E., Griffiths, R.E., Johnston, M.D., and Schwartz, J. 1979, Ap. J. (Letters), in press.

Snijders, M.J.A., Boksenberg, A., Barr, P., Sanford, P.W., Ives, J.C. and Penston, M.V. 1979, M.N.R.A.S., in press.

Snyder, W.A. et al. 1978, Ap. J. (Letters) 237, L11.

Sramek, R.A. and Tovmassian, H.M. 1976, Ap. J. 207, 725.

Stein, W.A., O'Dell, S.L. and Strittmatter, P.A. 1976, Ann. Rev. A. Ap. 14, 173.

Tapia, S., Craine, E.R., and Johnson, K. 1976, Ap. J. 203, 291.

Ulrich, M.-H., Kinman, T.D., Lynds, C.R., Ricke, G.H., and Ehers, R.D. 1975, Ap. J. 198, 261.

Weiler, K.W., and Johnson, K.S. 1980, preprint.

Worrall, D.M., Mushotzky, R.F., Boldt, E.A., Holt, S.S. and Serlemitsos, P.J. 1979, Ap. J., in press.

Yee, H.K.C., and Oke, J.B. 1978, Ap. J. 226, 753.

TABLE 1. INFORMATION ON OBSERVATIONS

Spectral Range	log ν	Other Units	Dates (1978)	Instrument
X-ray	19.08-17.68	50-2 keV	Aug. 21-31	HEAO-1 A2
	19.08-17.68	50-2 keV	Sep. 8, 9	HEAO-1 A2
UV	15.36-15.20	1275-1910 $\mathring{A}$	Aug. 25	IUE
	15.20-14.97	1900-3140 $\mathring{A}$	Aug. 26	IUE
Visible Light	14.96-14.42	3290-11410 $\mathring{A}$	Aug. 29, 30, 31	5-meter
IR	14.13	2.2 mμ	Aug. 31	2.5-meter
Radio	10.03	10650 MHz	Aug. 30 - Sep. 3	46-meter
	10.02	10275 MHz	Aug. 15-24	46-meter
	9.68	4750 MHz	Aug. 15-31	300-ft

FIGURE CAPTIONS

Figure 1 - The X-ray spectrum of MK 501 in 1978 Aug-Sept. The upper left panel shows the best fit power law spectrum folded through the detector response compared to the pulse height data. The lower left panel gives the incident spectrum unfolded using the best fit model. The lower right panel shows the 90% confidence contour for the X-ray power law index and the X-ray absorption in units of 10^{21} at/cm^2.

Figure 2 - Ultraviolet spectral energy distribution of MK 501 from IUE observations on 1978 August 25-26. Open circles represent data without correction for reddening. Solid circles indicate data corrected for reddening assuming E(B-V) = 0.083 mag. The points represent averages for frequency bins containing 10 points each, with error bars indicating $\pm$ 2σ internal error for the bin means.

Figure 3 - Absolute spectral energy distribution of MK 501 in visible light on 1978 August 30 through an aperture of diameter 10" on the 5-meter telescope.

Figure 4 - 46-meter radio observations of MK 501 at 10650(Δ) and 10275 (θ) MHz obtained on 1978 August 15 through September 3. Error bars on individual observations are $\pm$ 2σ. The dashed line indicates the mean flux density, 1.14 Jy.

Figure 5 - 92-meter radio observations of MK 501 at 4750 MHz obtained on 1978 August 14 through September 1. Error bars are $\pm$ 2σ.

Figure 6 - Combined absolute spectral energy distribution of MK 501 from X-ray to radio wavelengths based on the observations obtained in 1978 August - September.

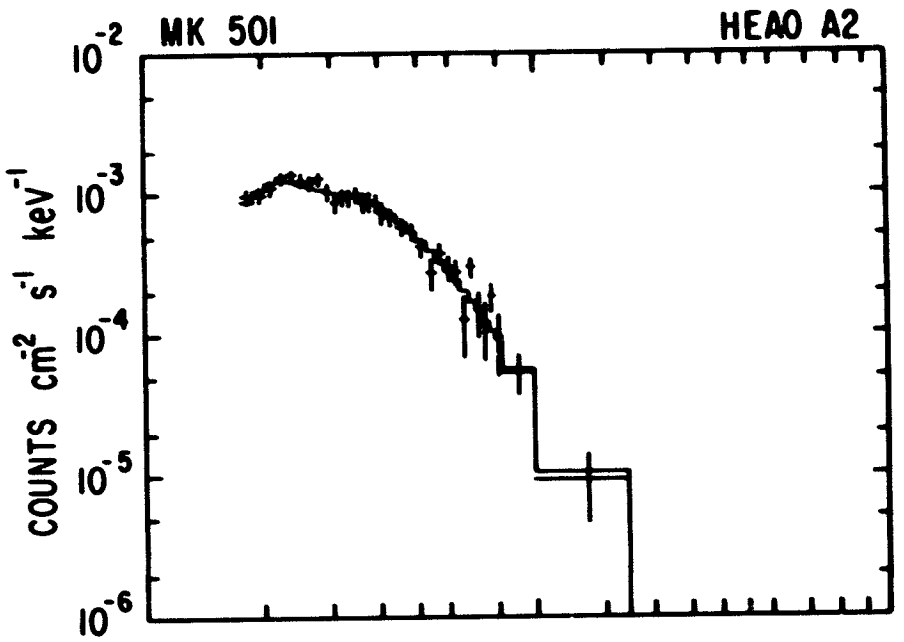

$AE^{-\Gamma}$ photons cm^{-2} s^{-1} keV^{-1}

$\Gamma = 2.52$

$A = 0.036$

$N_H = 4.6\ 10^{21}$ atoms cm^{-2}

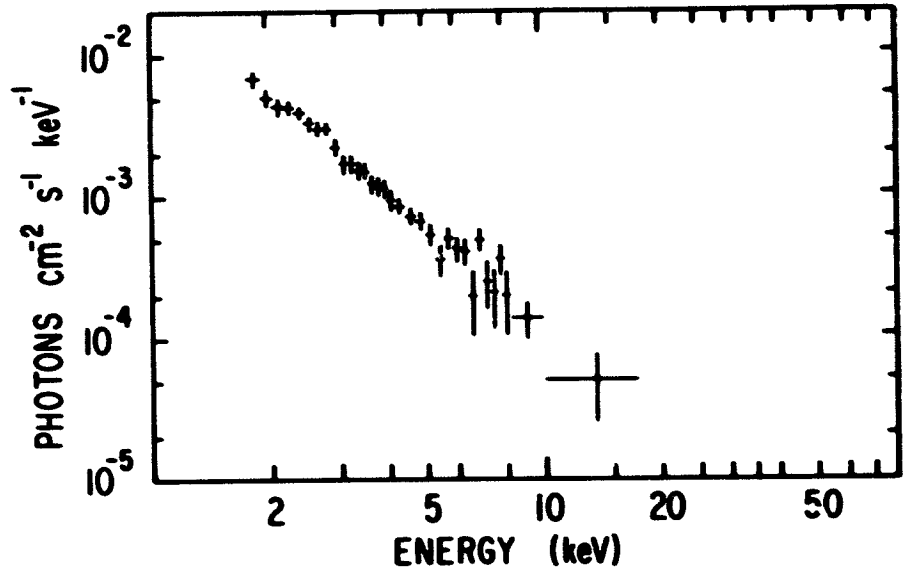

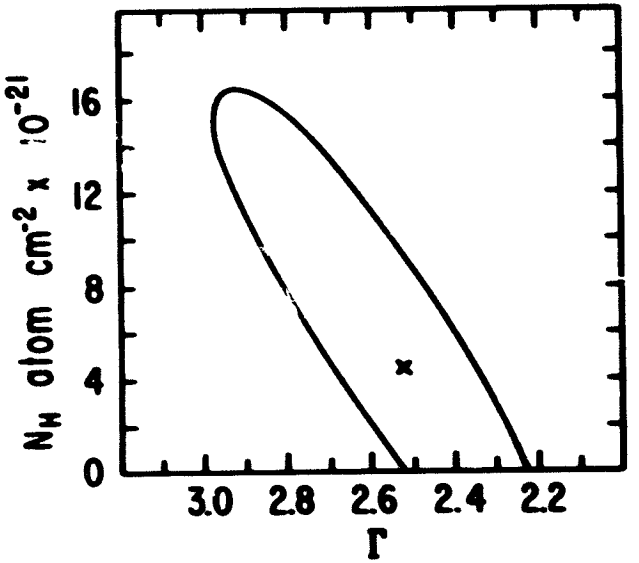

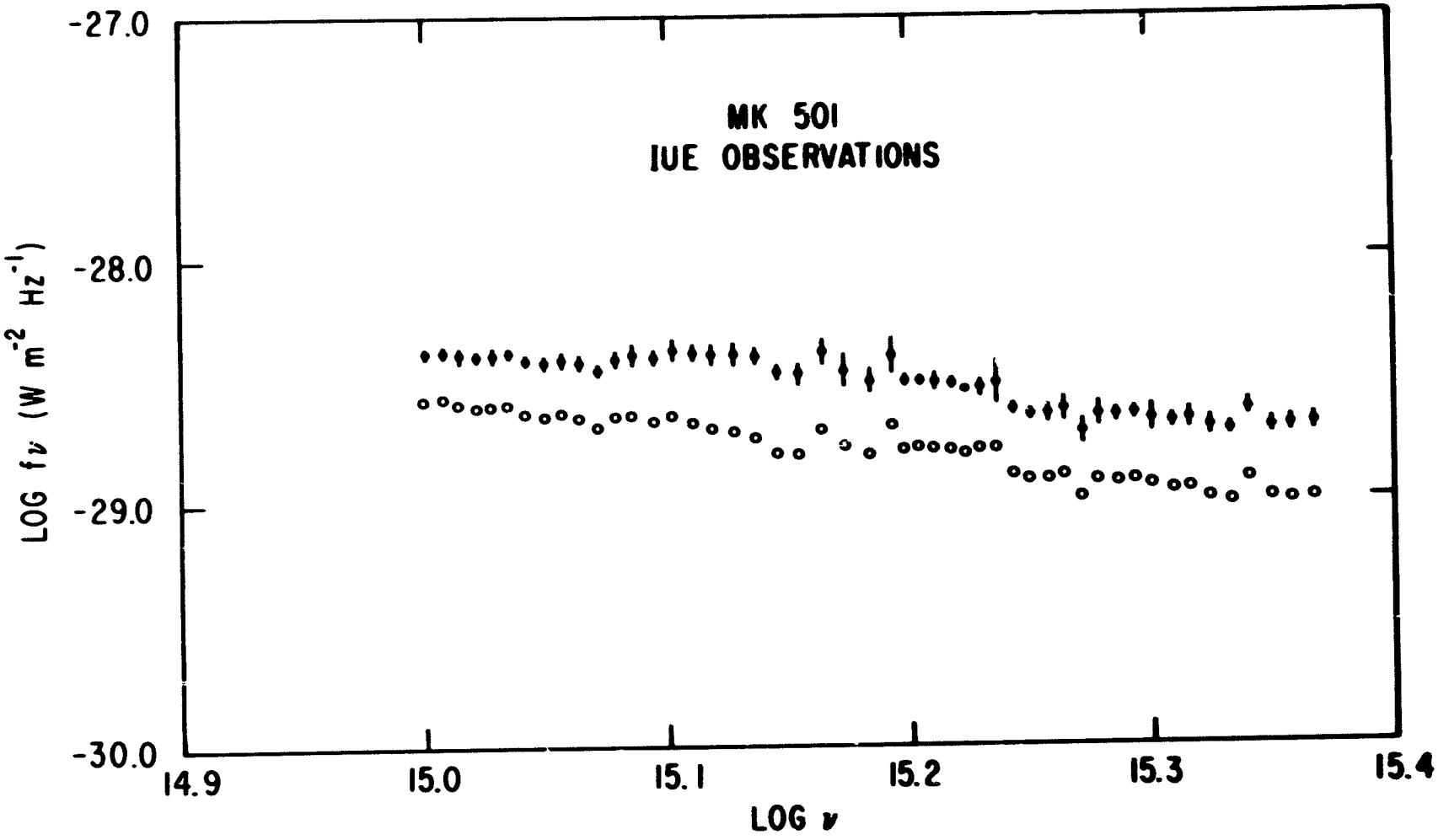
MK 501
IUE OBSERVATIONS
-27.0
-28.0
-29.0
-30.0
LOG fν (W m⁻² Hz⁻¹)
14.9
15.0
15.1
15.2
15.3
15.4
LOG ν

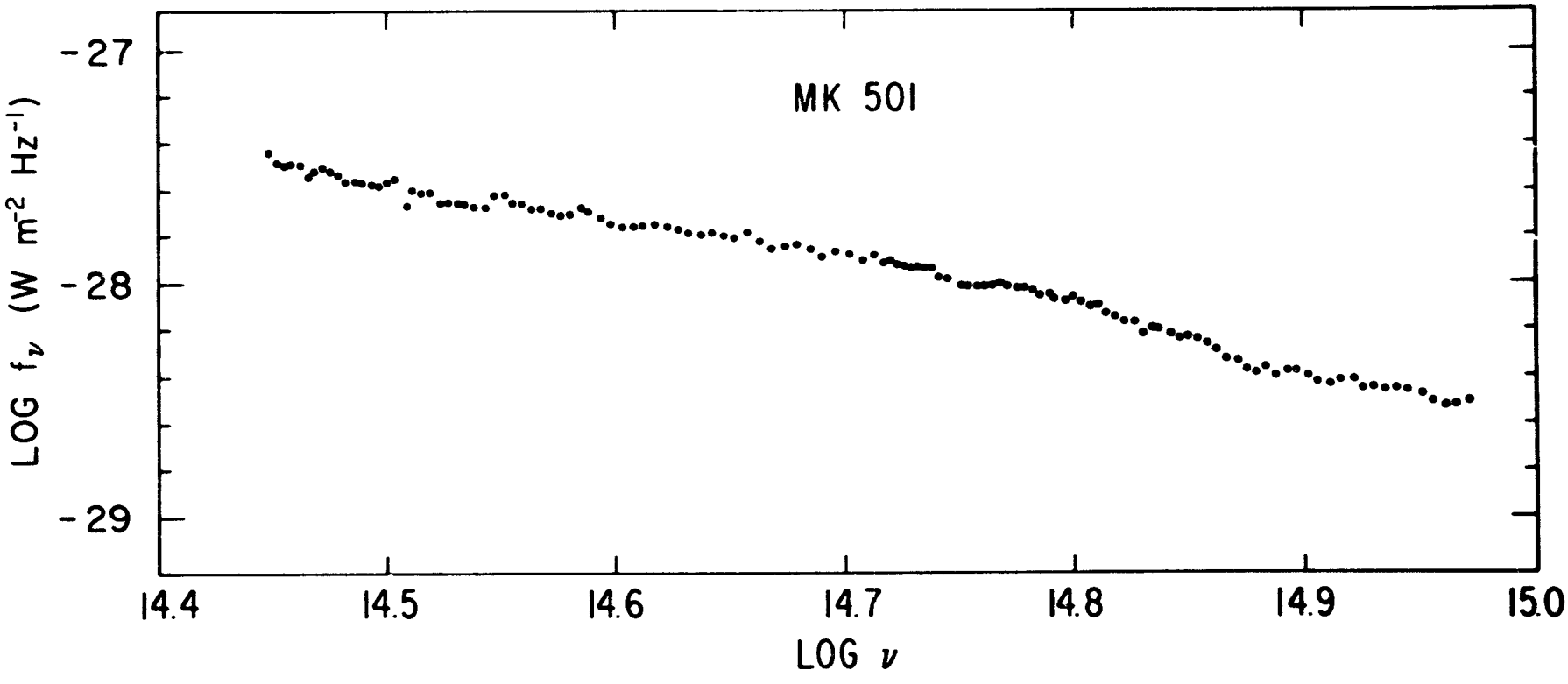
MK 501
-27
-28
-29
LOG f_ν (W m^{-2} Hz^{-1})
14.4
14.5
14.6
14.7
14.8
14.9
15.0
LOG ν

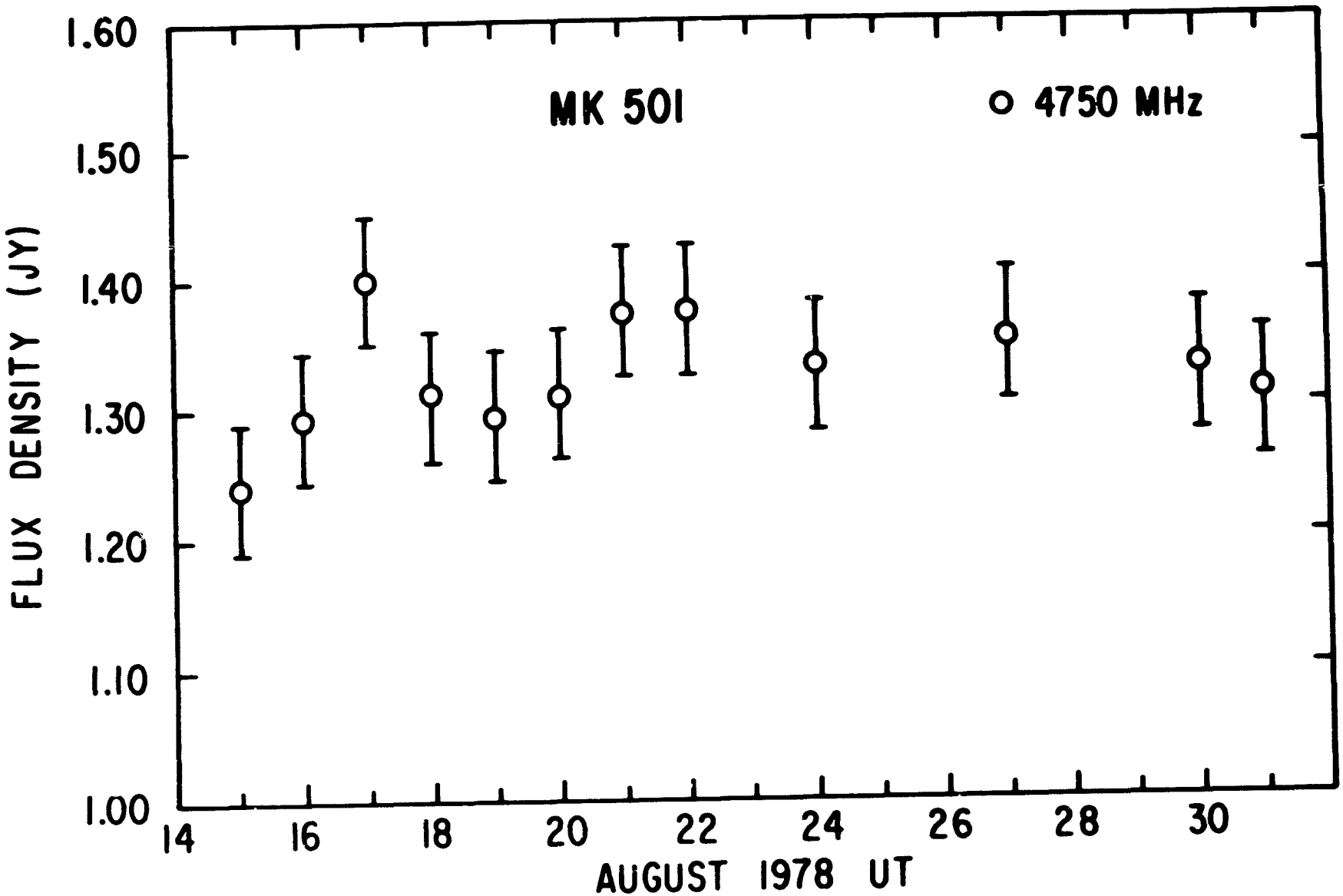
MK 501
o 4750 MHz
FLUX DENSITY (JY)
1.60
1.50
1.40
1.30
1.20
1.10
1.00
14
16
18
20
22
24
26
28
30
AUGUST 1978 UT

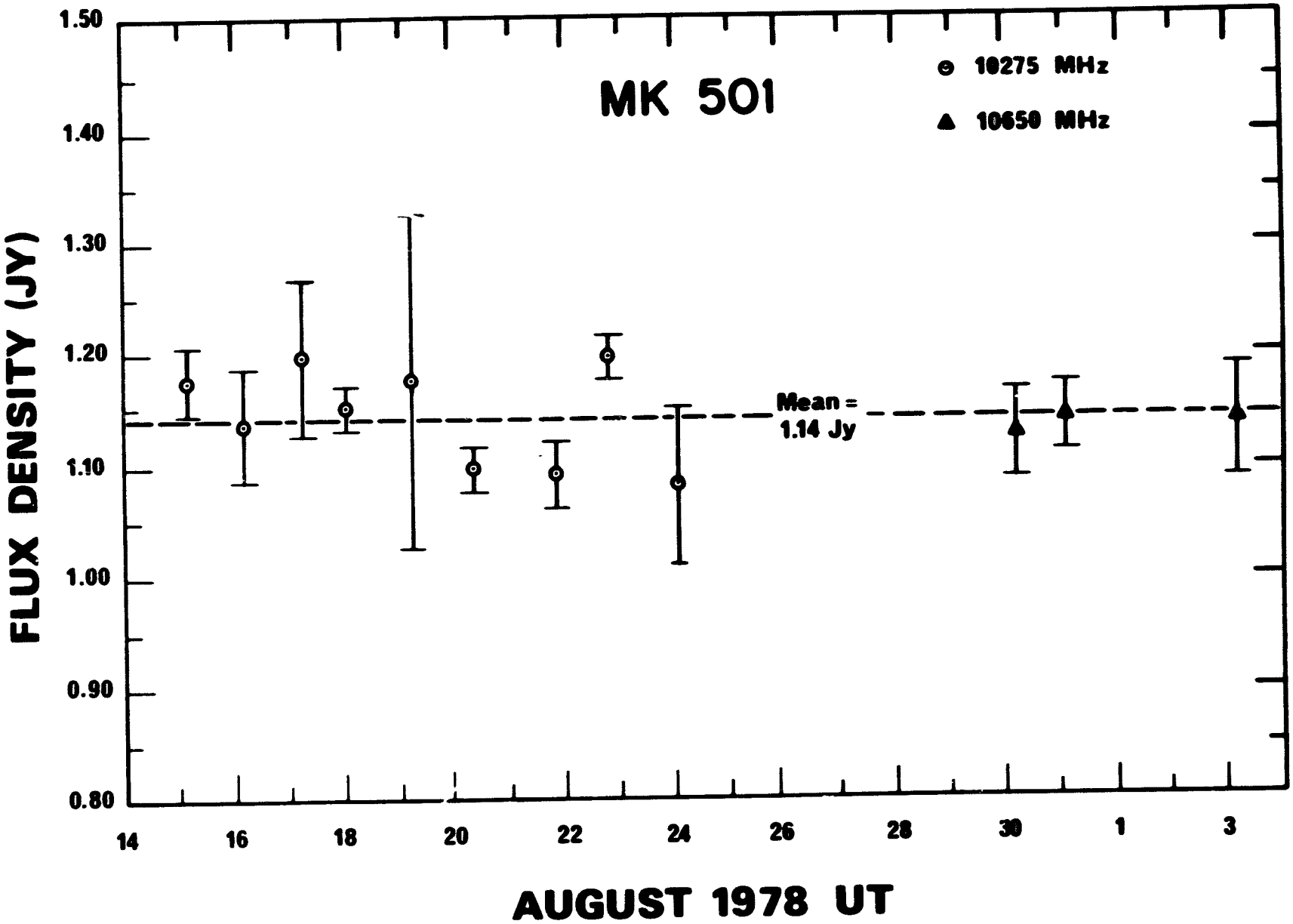
MK 501
10275 MHz
10650 MHz
Mean =
1.14 Jy
FLUX DENSITY (JY)
1.50
1.40
1.30
1.20
1.10
1.00
0.90
0.80
14
16
18
20
22
24
26
28
30
1
3
AUGUST 1978 UT

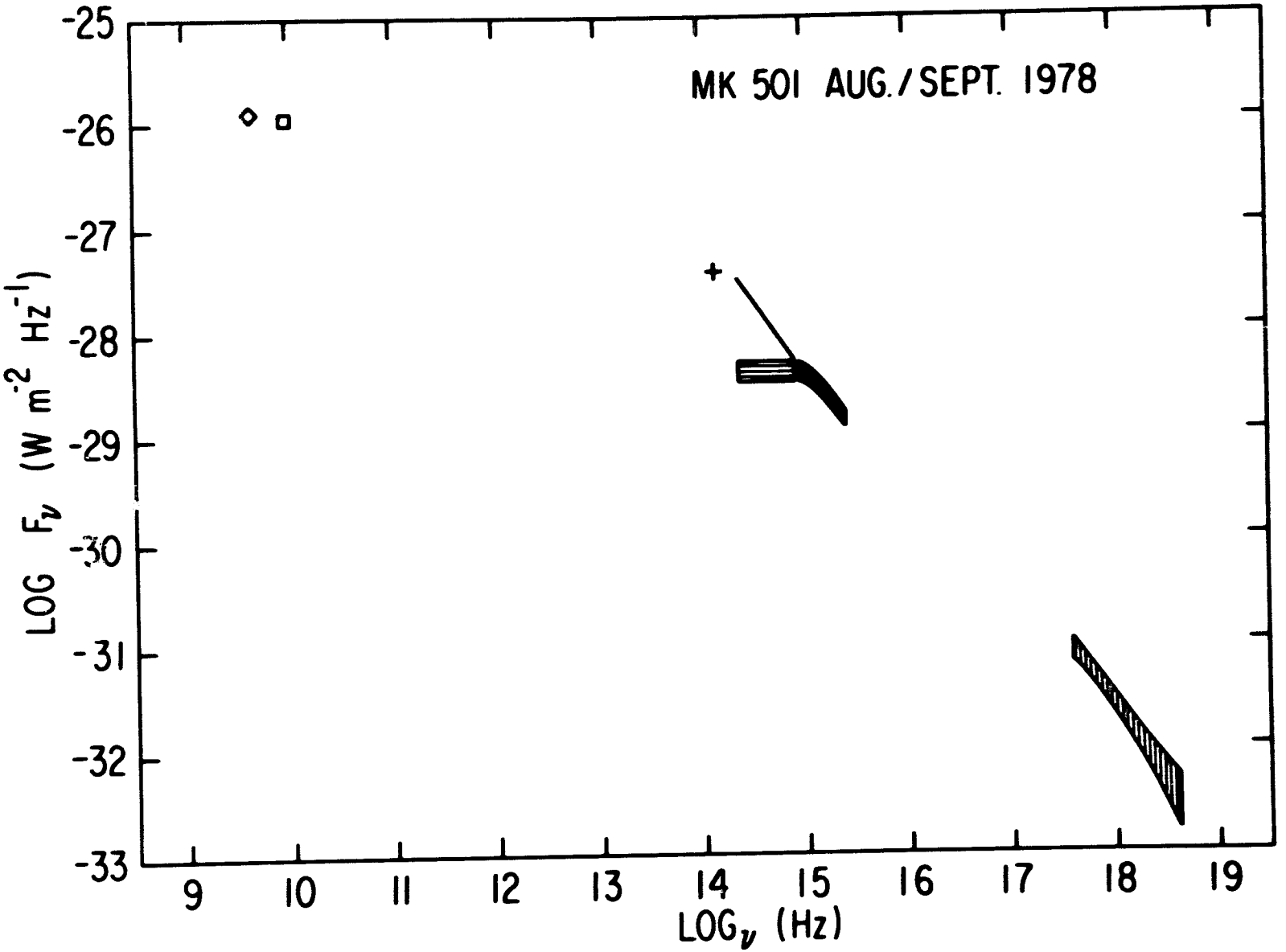
MK 501 AUG./SEPT. 1978
-25
-26
-27
-28
-29
-30
-31
-32
-33
LOG F_ν (W m^{-2} Hz^{-1})
9
10
11
12
13
14
15
16
17
18
19
LOG$_\nu$ (Hz)